nature ecology & evolution

Article

https://doi.org/10.1038/s41559-026-03042-0

Dynamics and ecology of a multistage expansion of Oropouche virus in Brazil

Received: 25 June 2025

Accepted: 19 February 2026

Published online: 17 April 2026

Check for updates

Houriiyah Tegally[1,53] ✉, Simon Dellicour[2,3,4,53], Jenicca Poongavanan[1,53], Carla Mavian[5,6,7,53], Graeme Dor[1], Vagner Fonseca[1,8,9], Massimiliano S. Tagliamonte[10], Marcel Dunaiski[11], Monika Moir[1], Eduan Wilkinson[1], Carlos Frederico Campelo de Albuquerque[12], Livia C. V. Frutuoso[13], Edward C. Holmes[14], Cheryl Baxter[1], Richard Lessells[15], Moritz U. G. Kraemer[16,17], José Lourenço[18], Luiz Carlos Junior Alcantara[9], Tulio de Oliveira[1,15,54] ✉ & Marta Giovanetti[19,20,54] ✉ on behalf of Consortium CLIMADE*

In March 2024, Brazil reported an unprecedented Oropouche fever outbreak, driven by the emergence of a reassortant lineage of the Oropouche virus (OROV) expanding beyond the Amazon Basin. To investigate the expansion dynamics of OROV, we implemented complementary phylogeographic and ecological niche modelling approaches that aimed to characterize the environmental factors associated with the range expansion and the risk of local circulation, respectively. Our analyses reveal a multiscale expansion process with both short- and long-distance dispersal events and diffusion velocities in line with air traffic-mediated jumps. We identify banana and cocoa cultivation, temperature, the predicted suitability of the primary vector *Culicoides paraensis* and human population density as key environmental factors associated with OROV range expansion in new areas. We further show that OROV circulated in areas of enhanced ecological suitability immediately preceding its explosive epidemic expansion in the Amazon. Our study provides valuable insights into the dispersal and ecological dynamics of OROV, highlighting the probable role of human mobility in the long-distance colonization of new areas and raising concern over high viral suitability along the Brazilian coast.

Oropouche virus (OROV)[1] is an arthropod-borne virus first identified in 1955 in Oropouche, a village in Trinidad and Tobago[1]. OROV causes a febrile illness[2] that can progress to severe neurological disease[1,3] and has been associated with maternal vertical transmission[4]. This re-emerging virus circulates primarily among wildlife, such as non-human primates and sloths, with antibody detections in rodents and birds[5,6]. During the last 60 years, OROV has caused around 30 documented human outbreaks in the Amazon region[7–10]. The midge *Culicoides paraensis* serves as the primary vector for human transmission[9,11,12], but other suspected secondary vectors include *Culex quinquefasciatus*[13–15], *Coquillettidia venezuelensis*, *Aedes (Ochlerotatus) serratus*[1,6], *Aedes aegypti*, *Aedes albopictus* and *C. quinquefasciatus*[15,16]. However, there is no evidence to date of vector competence in any mosquito species[17].

In March 2024, the Pan American Health Organization issued an alert in response to a rapid increase in Oropouche fever cases across several countries[18,19]. Brazil has been particularly affected, reporting not only the most cases, but also severe complications linked to OROV infection, including fatal cases[4,18,20], maternal and fetal impacts[21,22],

A full list of affiliations appears at the end of the paper. ✉e-mail: houriiyah@sun.ac.za; tulio@sun.ac.za; giovanetti.marta@gmail.com

with ~8,318 confirmed cases in Brazil alone as of epidemiological week 40 of 2024. Recent epidemiological data and genomic investigations in Brazil[23–27] have described the recent expansion of OROV into previously non-endemic regions and other states outside the Amazon Basin, where OROV had not been reported or had only sporadic detections in past decades. Some of these studies have identified reassortment events in the virus genome that may have contributed to its changing epidemiology[23–27]. While the exact role of reassortment in the adaptation of OROV to new environments remains to be fully understood, it has possibly impacted its spread into new ecological niches (that is, the ranges of environmental conditions suitable for the local circulation of the virus)[23–27].

As with other arboviruses[28], recent changes in ecological context, such as deforestation, urbanization, human mobility and climate change, have possibly contributed to the emergence of OROV in new regions[29]. In particular, environmental disruption pushes non-human mammal reservoirs and vectors into closer contact with human populations, facilitating viral spread[30]. Additionally, human activities[31,32] such as urban expansion and altered land use increase the risk of transmission of OROV to humans in sylvatic and peri-urban settings, where vectors such as *C. paraensis* thrive[33–35]. Recent studies have used phylogenetic methods to reveal the timing and spatial paths of the emergence and spread of $OROV_{BR\text{-}2015\text{-}2024}$ lineage in Amazonian subregions[23] or have investigated environmental factors linked with OROV transmission using the association of epidemiological data with land cover types[26,27]. Nonetheless, epidemiological, ecological and genomic data have not yet been analysed in an integrated way and much remains unknown about the broader disease ecology of OROV, particularly concerning environmental correlates of local circulation and of its recent geographical range expansion. This lack of comprehensive understanding hampers effective risk assessment and preparedness efforts, both in Brazil and across the Americas.

Our study aimed to test key epidemiological hypotheses regarding OROV disease ecology and its range expansion, both spatially and temporally, specifically: (1) that the dispersal history and dynamics of OROV in Brazil followed a multistep pattern over different time periods; (2) that recent changes in OROV distribution reflect a spatial redefinition of its ecological niche, with environmental suitability expanding from historically restricted Amazonian areas to newly permissive regions across Brazil; and (3) that subtle variations in *C. paraensis* suitability may have facilitated the recent expansion of OROV. We integrated georeferenced pathogen genomes, epidemiological and geospatial data through complementary analytical frameworks.

Results

Dispersal history and dynamics of OROV in Brazil

The epidemiological dynamics of OROV expansion in Brazil in late 2023 and 2024 show a two-stage process: a rapid rise in cases in Amazonian states, namely Acre, Amapá, Amazonas, Pará, Rondônia and Roraima, as well as parts of Mato Grosso and Maranhão, which together encompass most of the Amazon Basin, particularly centred around Manaus (capital of the state of Amazonas), followed by widespread circulation in other parts of the country (Supplementary Fig. 1). To investigate this epidemiological pattern, we applied a continuous phylogeographic approach using over ~500 genomes generated by previous studies[23,24] and sampled between 2022 and 2024. Building on prior knowledge of reassortment events across genome segments[23,24], we conducted separate phylogeographic reconstructions for segments L, M and S, acting as experimental replicates for downstream analyses. Our analysis extracted spatiotemporal dispersal information from the branches of 100 spatially explicit phylogenies subsampled from each post-burn-in posterior distribution, revealing new insights about OROV dispersal events between sampled regions, as detailed below (Fig. 1a).

The earliest lineage dispersal events were restricted to the Amazon basin and inferred to be before 2020, with the virus gradually spreading to other Brazilian states in a southeasterly direction in 2023 and 2024. The apparent discrepancies between the time inferred for the most recent common ancestor (tMRCA) of each segment (Fig. 1a) probably reflect slightly different evolutionary histories among those segments. Indeed, reassortment between genomic segments means that they have distinct genealogies. However, these tMRCA estimates are not substantially different as they have large overlapping 95% highest posterior density (HPD) intervals, which could also be related to the weak yet substantial temporal signal evaluated for those alignments (Methods; March 2017 to September 2020 for segment L, August 2016 to December 2019 for segment M and July 2015 to April 2018 for segment S). By further examining the spatial dissemination of OROV lineages across Brazil, we found that the virus reached a maximal wavefront distance (furthest extent of the wavefront from the location of the inferred tree root position) of over 3,000 km from its epidemic origin through the entire dissemination period (Fig. 1b). This reconstruction further captured two distinct expansion phases during which the wavefront distance increased rapidly, indicating the introduction into new areas in 2024 (Fig. 1b). The rapid expansion of the wavefront in 2024 corresponded to the increase in cases in areas outside the Amazon (Supplementary Fig. 1). Furthermore, diffusion coefficient estimates changed through time, with increases in the first 6 months of 2023 and 2024, corresponding to the expansion phases and consistently detected in all three OROV segments (Fig. 1c), reflecting a substantial dispersal capacity. In 2024, a non-negligible proportion of inferred lineage dispersal events occurred within the states of Mato Grosso, Minas Gerais and Bahia (~46%, ~45% and ~43% for segments L, M and S, respectively), that is some Brazilian states where there was no previous sustained OROV circulation.

When inspecting the association between the geographic distance (km) travelled by each phylogenetic branch and the associated diffusion velocity (km^2 per day) of the inferred lineage dispersal event, we observed a large group of phylogenetic branches associated with relatively short dispersal distance (<20 km) and slow diffusion (<4 km^2 per day; Fig. 1d), as well as a subsequent group of phylogenetic branches that correspond to faster long-distance dispersal events (that is, lineage dispersal events associated with notably high diffusion velocity; Fig. 1d). This supports a multiscale expansion process with a combination of short-distance dispersal events and fast long-distance jumps, with some of the latter probably reflecting human-mediated virus movements through air traffic. We also identified signals of substantial isolation-by-distance (IBD), with Pearson correlations between patristic and log-transformed geographic distances between samples close or greater than 0.5 for all three segments (0.470 (95% HPD = [0.360, 0.599]) for segment L, 0.575 (95% HPD = [0.286, 0.607]) for segment M and 0.684 (95% HPD = [0.326, 0.710]) for segment S); the patristic distance being defined as the sum of the branch lengths that link two tip nodes in a phylogenetic tree. Overall, these dispersal metrics provide a clear indication of rapid long-distance dispersal events during the recent OROV expansion in 2024 beyond the Amazon Basin, probably human-mediated through air travel, followed by more localized viral circulation.

Ecological factors associated with dispersal of OROV in Brazil

To investigate the ecological factors associated with the spatial expansion of OROV in Brazil, we analysed virus dispersal history in relation to 28 environmental factors (including land-use, climatic and demographic variables; Supplementary Fig. 2). This includes a species distribution model for *C. paraensis*, the recognized vector for OROV[1,9,11,12,36]. Using high-resolution environmental rasters for each covariate (Supplementary Fig. 2), we extracted environmental values at the geographic location of each phylogenetic node. These correspond to inferred positions through continuous phylogeographic analysis for internal nodes and to sampling locations (down to municipality level) for tip nodes (Supplementary Fig. 3). Specifically, we assessed shifts

https://doi.org/10.1038/s41559-026-03042-0

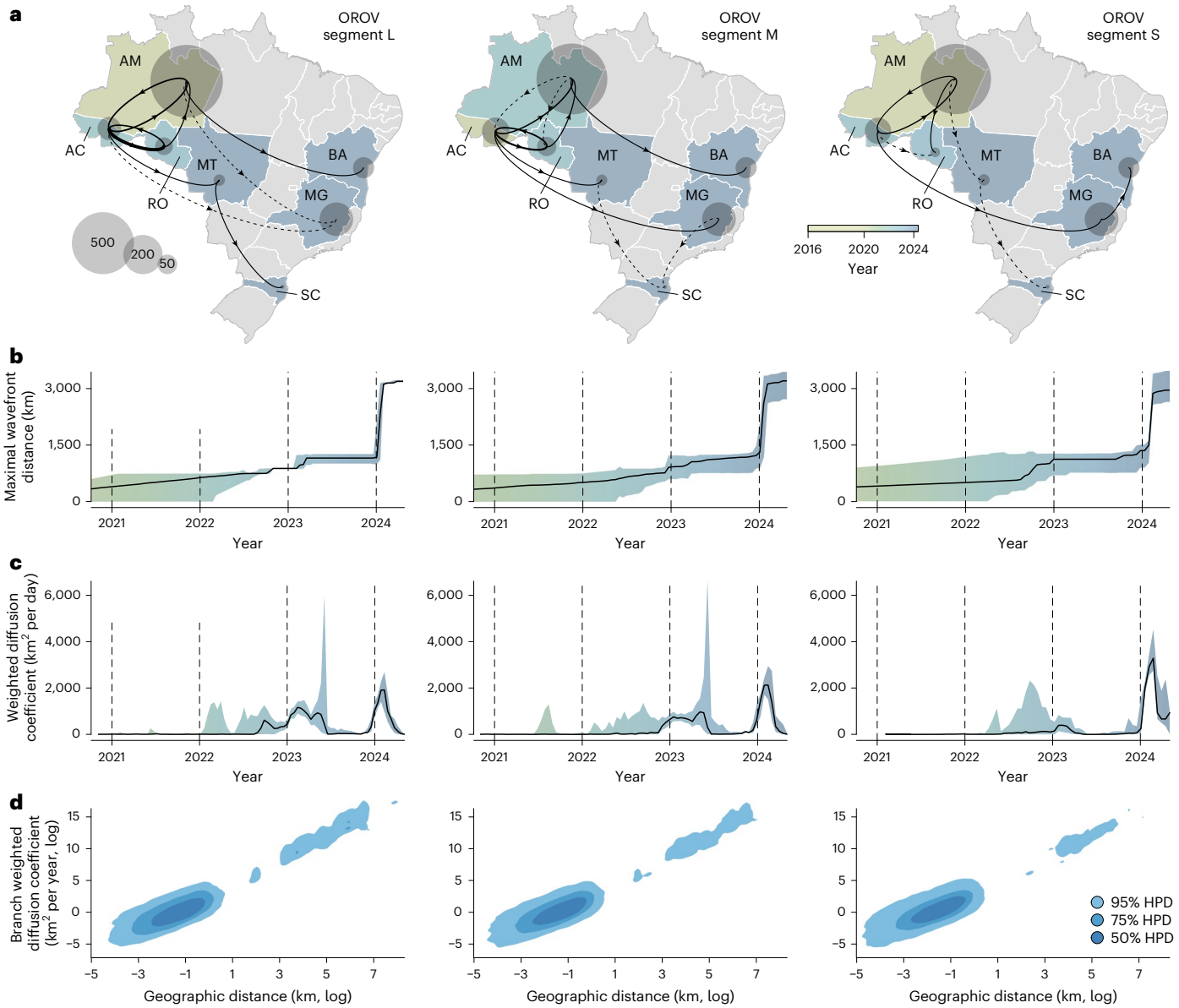

Fig. 1 | Dispersal history and dynamics of OROV lineages in Brazil. **a**, Dispersal history of OROV lineages inferred through continuous phylogeographic reconstructions. Lineage dispersal events between Brazilian states with a posterior probability ≥0.95 are shown by solid arrows and dispersal events with a posterior probability <0.95 are shown by dashed arrows. Additionally, the location of the different areas is represented by transparent grey dots whose surface is proportional to the number of local lineage dispersal events, that is phylogenetic branches inferred as remaining in that state. Brazilian states are coloured according to the estimated date of the first invasion event (median date computed from the 100 trees sampled from the posterior distribution) and are labelled with their abbreviated names (AC, Acre; AM, Amazonas; BA, Bahia; MG, Minas Gerais; MT, Mato Grosso; RO, Rondonia; SC, Santa Catarina). The tMRCA estimated for each segment are associated with large and overlapping 95% HPD intervals: from March 2017 to September 2020 for segment L, from August 2016 to December 2019 for segment M and from July 2015 to April 2018 for segment S. **b**, Evolution through time of the spatial wavefront distance, representing the maximal distance from the epidemic origin over time. The solid curve corresponds to the median estimate and the surrounding ribbon—coloured according to time—to the corresponding 95% HPD interval. **c**, Evolution through time of the weighted diffusion coefficient, a dispersal metric that measures the dispersal capacity of viral lineages. As in **b**, the solid curve corresponds to the median estimate and the surrounding ribbon to the 95% HPD interval. **d**, Kernel density plots with the branch-weighted diffusion coefficient against the geographic distance travelled by each branch (both axes being log-transformed). Base map derived from the GADM database, version 4.1 (https://gadm.org).

in dispersal environments relative to four specific periods: (1) before and (2) after the re-emergence and epidemic expansion in the Amazon (< and > mid-2023), (3) during the Amazon-restricted transmission phase (<2024) and (4) during the national expansion phase (>2024).

Before formally testing these associations, we first visually explored the temporal evolution of the environmental conditions associated with the dispersal locations of inferred lineages. For this purpose, we extracted and averaged the environmental values crossed by lineage dispersal during successive time slices of ~2 weeks and while considering a sliding window of ~1 month. These visual explorations indicate that, when comparing dispersal events before and after 2023–2024, different environmental conditions for OROV circulation are already noticeable (Fig. 2): certain dispersal environments seem to shift at the mid-2023 time point, while others at the 2024 time point (Fig. 2 and Supplementary Fig. 3). For instance, before 2024, dispersal events tended to occur in areas with relatively higher evergreen broadleaf forest cover and higher mean annual temperature (Fig. 2 and Supplementary Fig. 3). Interestingly, most lineage dispersal locations

https://doi.org/10.1038/s41559-026-03042-0

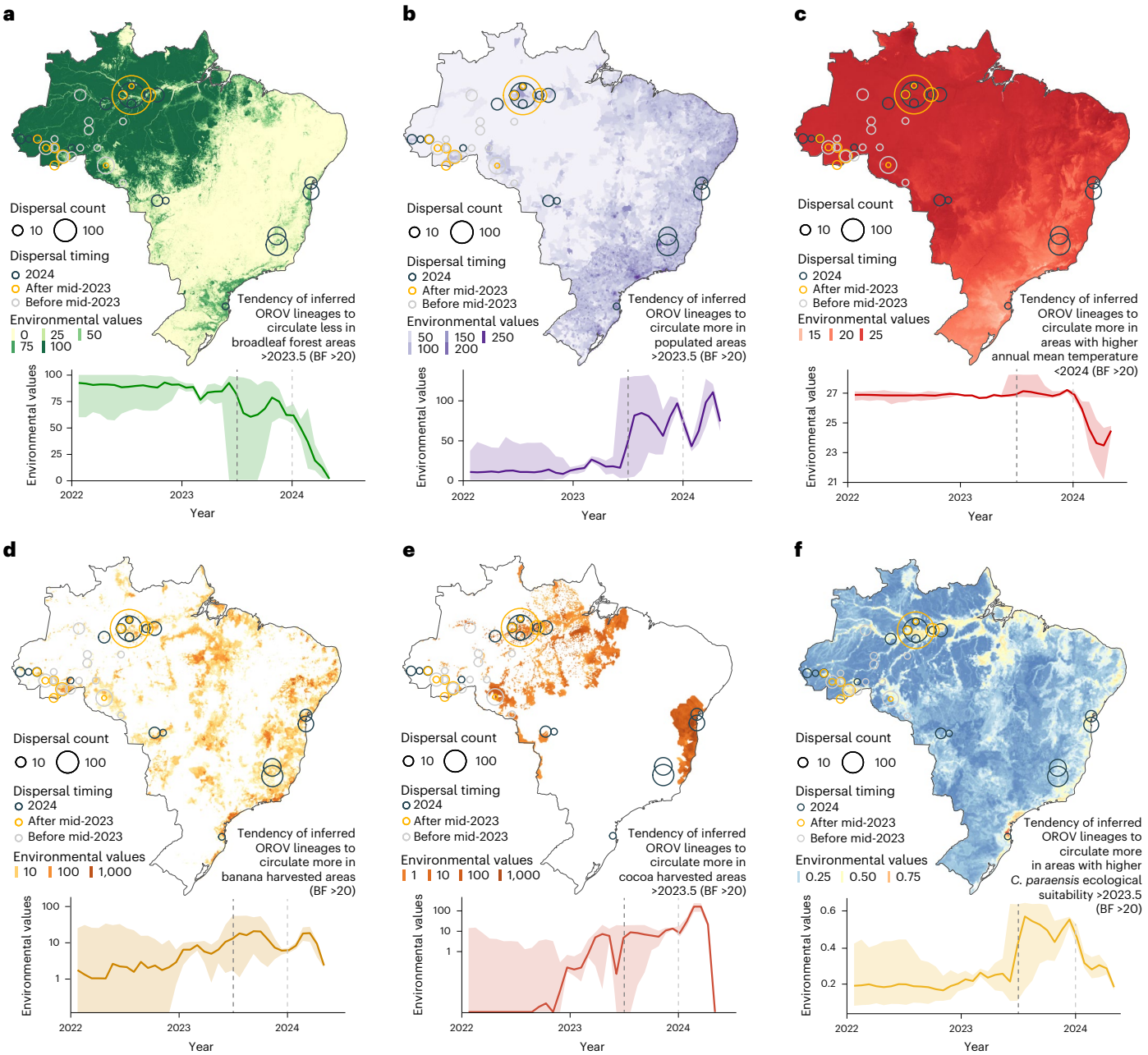

Fig. 2 | Environmental conditions associated with OROV lineage dispersal locations over time (for segment M). a–f, The spatial distribution of six main environmental factors (units specified): evergreen broadleaf forest cover (%) (**a**); human population density (normalized between 0 and 255 per km^2 for visual clarity) (**b**); mean annual temperature (°C) (**c**); banana-harvested area (in hectares, log-transformed) (**d**); cocoa harvested area (in hectares, log-transformed) (**e**); and *C. paraensis* ecological suitability distribution (probability of occurrence) (**f**), in the top rows. Circles on the map depict the end node of dispersal locations inferred by continuous phylogeography, sized by the number of lineage dispersal events in an area and coloured by the timing of the event. Bottom rows of each panel are line graphs, with solid curves and shaded ribbons representing median estimates and 95% HPD intervals, respectively, depicting the environmental covariates associated with the locations of OROV lineage dispersal events in Brazil. Each plot illustrates the change over time (2022–2024) of specific environmental conditions encountered by viral lineage dispersal events. The embedded statements summarize the results of the landscape phylogeographic analyses investigating the association between environmental conditions and the dispersal location of inferred OROV lineages. 'BF >20' refers to a BF value being considered as strong support, following the scale of interpretation of ref. 38. Base map derived from the GADM database, version 4.1 (https://gadm.org).

before 2024 were associated with a mean temperature of ~27 °C, which probably corresponds to the thermal optimum for OROV transmission suitability within our model, rather than the ecological optimum for *C. paraensis* abundance[37]. However, dispersal environments were already shifting towards areas with comparatively higher human population density and urbanization around mid-2023 (Fig. 2 and Supplementary Fig. 3). With strong Bayes factor (BF) support (>20)[38], our analyses demonstrated that these trends in dispersal environments were consistent across the posterior distribution of trees obtained through continuous phylogeographic inference.

To statistically test the association of environmental conditions with the spread of OROV lineages, we used a landscape phylogeographic approach to analyse the values extracted at the tree node positions for all 28 environmental factors considered in this study[39].

Specifically, for the four distinct time periods mentioned above (<mid-2023, >mid-2023, <2024 and >2024), we tested whether inferred OROV lineages tended to preferentially circulate in or avoid circulating in certain environmental conditions. Statistical support (BF) was obtained by comparing the results from phylogeographic reconstructions with a null dispersal model, in which a new continuous diffusion process was randomly simulated along the same tree topologies. During both transmission phases divided by the 2024 cut-off, our results reveal strong support (that is, BF > 20 for at least two out of three segments) for preferential circulation of inferred OROV lineages in areas with comparatively higher population density and urbanization, lower evergreen broadleaf forest cover, areas associated with cocoa cultivation and higher ecological suitability for the *C. paraensis* vector (Fig. 2 and Supplementary Table 1), which is also found in areas without banana and cacao plantations. We also found strong support for a preferential circulation of inferred OROV lineages in areas associated with banana cultivation in the expansion phase (>2024), as well as in the pre-expansion phase (<2024) for segment L (Supplementary Table 1). These results are consistent with existing knowledge about *C. paraensis* larvae developing in microhabitats of decaying debris from banana and cacao plantations[40–42]. Specific to the Amazon-only transmission phase (<2024), our results also reveal a preferential circulation in areas with comparatively higher mean annual temperatures (BF > 20; Fig. 2c). Of note, we also tested the association of forest loss with the OROV spread but it did not lead to strong support in any of the time periods considered. However, an examination of the environmental conditions associated with lineage dispersal locations between transmission phases before and after mid-2023 revealed compelling differences: for instance, for viral lineages inferred before mid-2023, there was no strong support for a preferential circulation of inferred OROV lineages in areas more ecologically suitable for the *C. paraensis* vector, areas associated with a comparatively higher mean annual temperature, lower evergreen broadleaf forest coverage and denser human populations, although there was still a preferential circulation in more urbanized areas (Supplementary Table 1). This suggests ecological differences underlying endemic OROV circulation within the Amazon before the re-emergence and rapid epidemic expansion at the end of 2023. Overall, our findings reveal similar trends across the three segments analysed (Supplementary Table 1).

Mapping ecological niches for OROV transmission and range expansion in Brazil

The rising number of human OROV detections provides an opportunity to apply modelling approaches to identify areas ecologically suitable for local virus circulation and potential human infections. We used an ensemble modelling approach to reveal OROV transmission suitability across Brazil. The suitability index ranges from 0 (unsuitable conditions) to 1 (highly suitable conditions) and illustrates the potential geographic areas where environmental conditions are most favourable for OROV transmission (Fig. 3a). The disease presence points used as model input represent OROV circulation leading to human cases from 450 geocoded sampling locations in Brazil (based on molecular testing and sequencing records) from 1957 to 2024 (~85% corresponding to 2023–2024). Given this large time span, climatic variables were matched to the corresponding decade of the occurrence point. In the context of presence-only ecological niche modelling, where true disease absence data are unavailable, we sampled pseudo-absence points. Pseudo-absence points sampling was informed by a kernel density estimate of human population density to reflect surveillance efforts, which we assumed is proportional to human population density, with an exclusion radius around presence points (Supplementary Fig. 4a). The model incorporated the same environmental covariates used in the landscape phylogeography analyses (Supplementary Fig. 1), while testing for overfitting along with model performance (Supplementary Table 3). A principal component analysis was performed to assess multicollinearity between the environmental covariates (Supplementary Fig. 4b), resulting in a final selection of eight variables: annual mean temperature, evergreen broadleaf forest cover, croplands cover, elevation, human population density, annual mean monthly precipitation, as well as cocoa- and banana-harvested area coverages. We also report variability among our model predictions as a measure of uncertainty (Supplementary Fig. 4c). Uncertainty is higher in the central regions of Brazil (Supplementary Fig. 4c), where limited surveillance and sparse sampling reduce the accuracy of our predictions. Overall, our findings indicate that the highest ecological suitability for local OROV circulation (>0.7) is concentrated in the northern regions (Fig. 3a), particularly within the Amazon Basin, which aligns with previous studies identifying this area as a significant epicentre for the virus[23,24]. Additionally, moderate- to high-suitability areas extend towards the northeast and central-western parts of Brazil, particularly in states such as Pará, Maranhão, Bahia and Mato Grosso, suggesting an expansion into previously non-endemic regions. Our model also highlights the potential for OROV transmission to move beyond traditional transmission range, affecting urban and peri-urban areas, particularly in the northeast (Fig. 3a), where human interaction with vectors may amplify transmission risks. This trend is especially notable for highly suitable areas around the coast of Brazil, where ~111.28 million people—corresponding to 54.8% of the population—reside (Fig. 2b). For cities situated within or near extensive forested areas, proximity to natural environments complicates the identification of precise exposure risks, as human–wildlife interactions and potential transmission events may occur in peri-urban areas, within the urban fringe or deeper within the surrounding forests.

To determine the individual contributions of each environmental factor to our ecological suitability prediction, we further calculated their relative importance (RI) in the resulting ecological niche models. We found that evergreen broadleaf forest cover and human population density contributed the most to the model predictions, followed by precipitation and banana and cocoa agricultural lands (Fig. 3d). This aligns with factors identified in the independent landscape phylogeographic analyses and provides important insights into the disease ecology of OROV. We plotted response curves to assess the relationship between the environmental factors and OROV transmission suitability. These curves illustrate how ecological suitability varies with changes in one factor while all others are kept constant at their mean. We observe a clear tipping point in ecological suitability with mean monthly precipitation, where environments with <2.5 mm mean monthly precipitation appear unsuitable for OROV transmission (ecological suitability ~0) whereas suitability increases considerably above this threshold (ecological suitability >0.4; Fig. 3d). For temperature, there is a clear increase in OROV suitability in environments with annual mean temperatures above 25–27 °C (Fig. 3d), reflecting ecological suitability for viral circulation rather than vector abundance. OROV transmission suitability decreases considerably at high elevations, while relatively higher human population density, evergreen broadleaf forest cover and higher areas of banana and cocoa agriculture appear to be associated with an enhanced risk of local OROV circulation (Fig. 3d).

To investigate whether the expansion of OROV in Brazil in late 2023 and 2024 was associated with an expansion of its ecological niche, we compared ecological niche models trained on pre-mid-2023, pre-2024 and all available occurrence records. Specifically, we compared both the resulting maps of OROV ecological suitability and the capacity of each category of models to predict the distribution of most recent occurrence data. The suitability ranges obtained with the pre-2024 models (Fig. 3b) highlight a similar spatial distribution of highly suitable regions compared with that obtained with the full models (Fig. 3a). While the full suitability estimates show a slight expansion of suitable areas, the pre-2024 model was able to predict the 2024 occurrence points with a relatively high performance (true skills statistic (TSS) = 0.60, area under curve (AUC) = 0.85; Supplementary Table 2). However, the pre-mid-2023 suitability range

https://doi.org/10.1038/s41559-026-03042-0

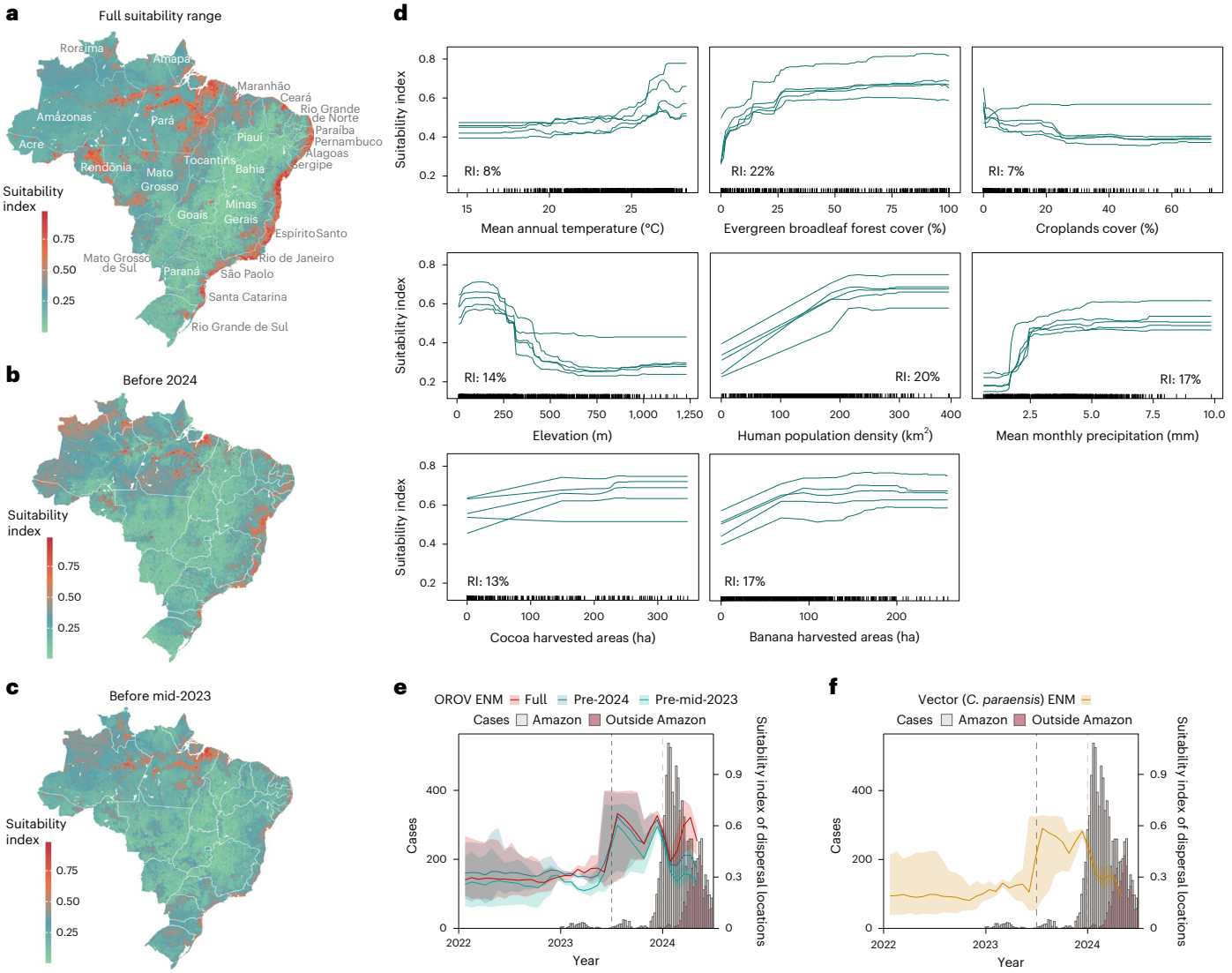

Fig. 3 | Ecological niche prediction for the risk of local OROV circulation in Brazil. a, Predicted ecological suitability for local OROV transmission across Brazil using the ensemble model with all available disease occurrence points. Ecological suitability predictions range from unsuitable (0) to highly suitable (1). **b**, Ecological suitability prediction from the ensemble model using input disease occurrence points sampled before 2024. **c**, Ecological suitability prediction from the ensemble model using input disease occurrence points sampled before mid-2023. **d**, Response curves and RI for individual environmental factors obtained from the RF suitability prediction model, which was the best-performing algorithm in the ensemble model. These response curves (five iterations) depict the relationship between the environmental factors and the response (the ecological suitability for local OROV transmission). **e**, OROV ecological suitability values associated with OROV lineage dispersal locations (for segment M) overlayed on weekly recorded OROV cases in Brazil. Suitability values are estimated from three ecological niche models, as described in the text. **f**, Vector ecological suitability values associated with the dispersal locations of OROV lineages (for segment M) overlayed on weekly recorded OROV cases in Brazil. Ecological suitability values are also shown for the vector *C. paraensis*. Shaded ribbons represent 95% HPD intervals. Base map derived from the GADM database, version 4.1 (https://gadm.org).

(Fig. 3c) shows clear differences from the full model, particularly in the landscape of ecological suitability within the Amazon; and the models had a lower predictive ability for occurrence points sampled after mid-2023 (TSS = 0.47, AUC = 0.76; Supplementary Table 2). While some of this effect could be due to the limited sample size of the pre-mid-2023 data (n = 89), this also suggests a shift in ecological suitability after mid-2023, associated with OROV amplification within the Amazon, before circulation in other parts of the country. This shift could have facilitated viral circulation outside the Amazon, which was probably associated with OROV lineages recently reaching areas that were newly ecologically suitable for local OROV transmission. This is supported by our earlier findings of long-distance and rapid-dispersal events from continuous phylogeography.

Integrating results from the ecological niche modelling with the inferred dispersal histories, we further assessed the estimated viral and vector ecological suitability at each dispersal location associated with OROV circulation across space and time (Fig. 3e,f). Examining viral lineage dispersal locations inferred before mid-2023, after mid-2023 and in 2024, it appears that for most of its dispersal history, sampled OROV lineages circulated in regions of moderate viral and vector ecological suitability (~0.4–0.5), consistent across the three temporal models we estimated and the viral and vector ecological niche models (Fig. 3e,f). This was then followed by a peak in both viral and vector ecological suitability values, reaching ~0.6–0.8 associated with OROV dispersal from mid- to late-2023, coinciding with unprecedented epidemic expansion within the Amazon (Fig. 3e,f and Supplementary Fig. 1). This peak in ecological suitability was probably a result of the virus being introduced to areas of the Amazon that had a combination of favourable environments and relatively higher population densities, such as Manaus, leading to an amplification of transmission. This expansion

in a highly suitable and more densely populated environment, in turn, probably facilitated the spread of the pathogen beyond its usual transmission range. This further emphasizes the need for improved surveillance in blind-spot regions where transmission suitability is high, but where cases may be under-reported or genomic data are scarce. In such regions, introductions could rapidly lead to amplified outbreaks. After 2024, ecological suitability associated with dispersal locations of sampled viral lineages became more variable, with values either remaining high (in the full OROV ecological niche model) or declining again (in the past OROV and *C. paraensis* ecological niche models). This variability is probably caused by the virus expanding into new areas, including those with less favourable environmental conditions (for example, lower mean annual temperatures—Fig. 2d, higher elevation and lower precipitation—Supplementary Fig. 3), despite relatively high population densities. In fact, the city of Manaus is situated within the Amazon rainforest, a unique characteristic that differs significantly from the primarily rural areas where OROV expansion has been observed.

Discussion, limitations and conclusions

The recent emergence and expansion of OROV into previously non-endemic regions in the Americas underscores the critical need for a deeper understanding of the factors associated with its spread. In response to the 2023–2024 outbreaks, recent studies have described the emergence of a reassortant lineage[23,24], investigated spatiotemporal movement dynamics at a smaller scale[18,19,23,24], reported severe clinical outcomes[4] and documented biological differences in the new lineage[43]. Some studies have investigated the ecological factors associated with the local circulation of OROV in parts of the country using epidemiological data[26,27], but not while also integrating insights from its recent dispersal history outside the Amazon Basin. Overall, large gaps remain in our understanding of the sudden large dispersal expansion beyond the Amazon[44].

Compared with previous approaches, our study provides an integrative analytical framework to examine how ecological factors may be associated with viral dispersal characteristics derived from phylogeographic reconstructions. This design enables us to explore these associations in a time-varying manner across the growth of the epidemic. We complement this with ecological niche modelling, a well-established method for assessing the spatiotemporal distribution of suitable environments for target organisms, including viruses. However, ecological niche models are observational tools with inherent limitations, especially for populations expanding into new environments that may not yet fully occupy their ecological niche. Their outputs should therefore be interpreted cautiously and ideally in combination with additional lines of evidence. Integrating phylogeographic and ecological niche modelling analyses provided complementary perspectives that allow us to address two related but distinct questions: the potential influence of environmental covariates on viral lineage dispersal dynamics and the ecological suitability associated with the risk of local viral circulation. Accordingly, for the first time we provide estimates of the strength of association of covariates using two methodological approaches, with hypothesis testing performed with genomic data, including previous comprehensive OROV genomic datasets beyond the Amazon region[18,19,23,24] and in a time-varying manner to test the timing of the association of different environmental factors with the OROV range expansion. Unlike previous investigations that focused either on spatiotemporal lineage movements within the Amazon or limited phylogenetic placements outside endemic regions[18,19,23,24],and others exploring environmental factors impacting OROV through associations between epidemiological data with land cover[26,27], our integrative approach explicitly combines phylodynamic reconstructions with ecological niche modelling to formally test associations between environmental factors and OROV dispersal. This combined framework enables a national-scale perspective and provides complementary insights into both the timing of viral expansion and the ecological conditions shaping it.

Environmental conditions play a pivotal role in shaping OROV transmission dynamics[45]. Zones undergoing land cover transitions, particularly those involving deforestation and agricultural activities, have emerged as hotspots for virus spread[46,47]. As these areas transition from sylvatic (forest) environments to more urbanized or agricultural landscapes, the resulting habitat changes bring vectors and reservoir hosts into closer contact with human populations, creating new opportunities for OROV transmission and these must be studied using an integrated approach[48]. Overall, the results of our analyses of environmental factors were consistent across both the phylogeographic and case-based ecological niche modelling frameworks. A notable exception was broadleaf forest cover, which exhibited a negative association in the phylogeographic approach but a positive association in the ecological niche modelling analyses. This contrast could potentially reflect a dynamic in which deforestation in areas of high forest cover create ecological conditions that facilitate OROV transmission. In this context, forest cover would then exhibit opposing associations depending on whether the signal captures dispersal dynamics—where forest loss may be more influential—or local circulation, where remaining forest cover may provide suitable habitats for vectors and increase opportunities for human exposure.

Through the landscape phylogeographic and ecological niche modelling analyses conducted in this study, we propose a mechanism for the expansion of OROV, first within and then beyond the Amazon. We detect shifts in ecological suitability and differences in the environmental space associated with dispersal events preceding epidemic amplification within the Amazon. Our findings support a two-step expansion process, in which circulation within a highly suitable environment led to a rapid outbreak in the Amazon, subsequently facilitating spread beyond the usual transmission range. This pattern is supported by independent reconstructions of all three genomic segments of the virus. While previous studies have identified the Amazon region as the primary source of OROV emergence in Brazil[23,24], re-emergence or introduction of the reassortant lineage in the vicinity of Manaus probably exposed a large human population and contributed to outbreak amplification. Higher suitability in this zone may reflect a combination of favourable environmental conditions and relatively denser human populations within the Amazon. Our results further suggest that circulation of OROV in non-endemic regions of Brazil may be self-limiting, particularly in less favourable environments.

More broadly, our study highlights the value of integrating phylodynamics and ecological niche modelling to investigate eco-epidemiological dynamics of re-emerging arboviruses and urban amplification. Using complementary analytical approaches and a comprehensive genomic dataset, we identify key environmental factors associated with OROV transmission. Both approaches implicate higher human population density and temperature, as well as banana and cocoa cultivation, as factors associated with OROV dispersal and circulation, consistent with previous findings[26]. These insights can inform public health planning and mitigation measures, including targeted vector control around agricultural areas near urban centres. While not confirmatory, our findings indicate that OROV expansion was associated with increasingly favourable and well-connected environments. Genomic reassortment may have contributed to enhanced transmission efficiency or immune escape, as suggested by prior hypotheses. The concentration of high-suitability areas in coastal regions of Brazil is of particular concern, given dense populations and the cocirculation of several arboviruses. Repeated introductions into these areas could lead to further amplification, especially in immunologically naive populations or in the presence of variants capable of immune evasion[43]. Transport infrastructure probably also shapes OROV spread, particularly in the Amazon region where roads and waterways act as major mobility corridors. Several suitable regions, especially in the northeastern and central-west areas, remain surveillance blind spots,

underscoring the need to prioritize active surveillance for early detection and outbreak prevention.

This study needs to be interpreted in light of several limitations. Our landscape phylogeographic approach is affected by the pattern of the sampling effort, as approximately half the node locations are sequenced tips, making them prone to sampling biases[39]. This means that this approach cannot currently test the true drivers of transmission but rather tests the strength of associations of dispersal environments. Additionally, we lack a species distribution model for vertebrate host species (for example, sloths) that typically compose the natural reservoir of OROV, which limits our ability to fully understand host–vector-specific environmental suitability. To mitigate this bias, we test associations against a null dispersal model generated through simulations and only consider factors with the strongest BF support (>20). Also of note was that this study was designed to only examine the environmental factors associated with dispersal expansion in Brazil, such that the potentially critical role of reassortants in viral adaptation and fitness was not addressed here. Our phylogeographic analyses focused solely on the reassortant lineage that emerged in Brazil. To elucidate the role of these evolutionary processes in the ability of the virus to adapt to new niches, hosts or vectors, our approach could be extended to analyse evolutionarily distinct lineages of OROV that previously circulated in Brazil or neighbouring regions. Vectors could also have played a central role in the recent range expansion of OROV, with the primary vector, *C. paraensis*, potentially adapting to new landscapes. Yet, the limited data on this species and the lack of direct evidence of such adaptation highlight the need for a more systematic surveillance to better characterize the distribution of *C. paraensis*. Moreover, ecological niche models are constrained by the availability and representativeness of georeferenced data and should therefore be interpreted cautiously. The interaction between the virus, its vectors and its reservoir hosts is crucial for both the colonization of new transmission zones and the maintenance of transmission in established areas. Finally, while deforestation has been discussed as a potential driver of the 2023–2024 OROV outbreak, in our analyses we did not find strong support for an association between forest loss and viral lineage dispersal locations. However, this absence of supported association should not be interpreted as evidence that forest loss is unimportant for OROV transmission. Rather, its effect may already be captured through correlated land-use variables in our models, particularly agricultural expansion. This may also reflect time-lags between forest cover loss and downstream impacts or limitations in the spatiotemporal resolution of the available data to fully capture these dynamics.

The geographic expansion of OROV into new regions highlights the pressing need for integrating environmental monitoring into public health frameworks. To effectively predict and mitigate the risks posed by OROV and other arboviruses, surveillance efforts must account for the complex interaction between environmental changes, vector ecology and human behaviour. As OROV continues to adapt to new ecological niches, potentially driven by combinations of genetic evolution and both natural and anthropogenic factors, a deep understanding of these dynamics will be essential for developing targeted intervention strategies to control its spread and minimize its public health impact.

Methods

OROV genomic data

Complete genome sequences of the S, M and L segments of the OROV, obtained from the first extra-Amazon OROV cases reported in the states of Bahia (northeast Brazil), Minas Gerais (southeast Brazil), Mato Grosso (midwest Brazil) and Paraná (south Brazil), were analysed together with corresponding segments from recently published full-length OROV genomes belonging to the Brazilian 2022–2024 sublineage[24]. The OROV sequences used correspond to GenBank accession IDs PQ168520–PQ247806 and PP153945–PQ065491. For each genomic segment (n = 545), several sequence alignments were generated using MAFFT[49,50] and subsequently manually inspected and curated in AliView[51] to remove sequencing artefacts and alignment errors. To ensure appropriate quality control for downstream evolutionary analyses, genomic regions identified by RDP5[52] as having probably arisen through recombination or reassortment were systematically excluded from the analyses. Specifically, these regions were masked by replacing the corresponding alignment positions with gap characters ('–'), resulting in genome alignments that explicitly exclude recombinant or reassortant signals, following previously established and validated approaches[52]. Sequences exhibiting extensive recombination or reassortment across most of the genome were excluded from further analyses (n = 43 for segment S and n = 1 for segment L). The resulting masked alignments were used for all downstream evolutionary and phylodynamic analyses.

Disease occurrence data

Disease occurrence data were compiled from several sources. Epidemiological data on OROV cases were retrieved from the Brazilian Ministry of Health, accessible at https://www.gov.br/saude/pt-br/assuntos/saude-de-a-a-z/o/oropouche. The dataset includes confirmed case reports from all Brazilian states where OROV cases have been notified, including but not limited to Acre, Alagoas, Amazonas, Bahia, Ceará, Minas Gerais, Pará, Rio de Janeiro and São Paulo. The data cover the years 2023 and 2024, organized by epidemiological week and include key variables such as the municipality, state, year of occurrence and the corresponding epidemiological week of reporting. These data were geocoded at the municipality level and occurrence deduplicated by month. Additional OROV occurrence data were gathered and geocoded from all records on the Global Biodiversity Information Facility (years 1957 to present) and GenBank (years 2015 to present) databases. After deduplicating all occurrence records, we obtained a total of 450 unique sampling location points covering the years 1957 to 2024, with most (~85%) sampled in 2023–2024.

Geospatial data

We tested several environmental factors both as associations with viral dispersal locations and as covariates in our ecological niche model. These factors included human population density, main land cover and climatic variables within the study area (Brazil). Each environmental factor was described by a raster that defines its spatial heterogeneity. Supplementary Table 3 details the source and resolution of each original raster file. In particular, the *C. paraensis* distribution map was obtained from previous work which used 78 cleaned occurrence points from Brazil to fit a random forest (RF) model (TSS = 0.687). Key predictors of suitability included banana- and sugarcane-harvested area, humidity, soil moisture and cassava-harvested area[35,53]. Each raster was cropped to match our study area (Brazil) by using Brazil shapefiles from the "rnaturalearth" package in R.

Phylogeographic reconstruction and lineage dispersal statistics

To model the spatiotemporal spread of OROV using spatially explicit phylogeographic reconstruction using the continuous diffusion model implemented in the software package BEAST 1.10[54], we used three different data subsets containing the 2022–2024 OROV sequences from various regions of Brazil of the S (n = 501), M (n = 545) and L (n = 544) segments. Before conducting the phylogeographic analyses, we assessed the strength of the molecular clock signal in each data subset using the root-to-tip regression method available in TempEst v1.5.3[55]. Preliminary BEAST reconstructions revealed an outgroup of sequences which diverged from the main clade ~60 years ago for each segment; these were subsequently discarded from our analyses. Temporal signal was evaluated for the resulting datasets yielding to correlation coefficients close to or above 0.5 (S, 0.4972; M, 0.635; L, 0.5123),

which corresponds to a weak yet substantial temporal signal. We reconstructed the spread of OROV lineages within Brazil by using a flexible relaxed random walk (RRW) diffusion model[56], which accommodates branch-specific variation in dispersal rates, with a Cauchy distribution and a jitter window size of 0.01 (ref. 57). The latitude and longitude coordinates of each sample were used in this analysis. Markov Chain Monte Carlo analyses were run in BEAST v1.10.4, with chains of up to one billion iterations each, sampling every 100,000 steps in the chain. The chains were stopped when convergence was reached following the removal of burn-in states. Convergence of each run was assessed using Tracer v.1.7.1, ensuring that the effective sample size for all relevant model parameters was >200 (ref. 58). Maximum clade credibility trees were retrieved and annotated using TreeAnnotator after discarding burn-in samples, the number of which was also determined in Tracer. Finally, the R package "seraphim"[59] was used to extract and map the spatiotemporal information embedded in the posterior trees. We further used "seraphim" to estimate three dispersal statistics from these movement vectors for each segment: maximal wavefront distances, weighted diffusion coefficients[60], measuring the dispersal capacity of viral lineages and an IBD signal measured as the Pearson correlation between the patristic and log-transformed geographic distances computed for each pair of tip nodes[61].

Landscape phylogeographic analyses

To investigate the association between environmental conditions (Supplementary Fig. 2) and dispersal locations of inferred OROV lineages, we first conducted a visual exploration and then formally tested these associations using a landscape phylogeographic approach[39]. For the visual exploration, we reported the environmental values explored by phylogenetic branches using the "spreadValues" function implemented in the R package "seraphim"[57]. Specifically, this function extracts and averages the environmental values crossed by the phylogenetic branch segments occurring during each successive time slice; and this individually for several trees sampled from the post-burn-in posterior distribution of trees inferred by each segment-specific continuous phylogeographic analysis. We here considered 100 posterior trees from each phylogeographic analysis, 200 time slices each spanning ~2 weeks from early July 2015 to early May 2024, as well as a sliding window of ~1 month.

To assess the tendency of inferred viral lineages to preferentially circulate within or avoid circulating in specific environmental conditions, we then compared the distribution of mean environmental values extracted at node positions in inferred trees ($E_{estimated}$) with those extracted at node positions in trees whose dispersal history had been resimulated under a null dispersal model ($E_{simulated}$). To generate such a null dispersal model, an RRW diffusion process was simulated along each tree topology used for the phylogeographic analyses. These RRW simulations were performed using the "simulatorRRW1" function of the R package "seraphim" from the sampled precision matrix parameters estimated by the phylogeographic analyses. Simulations conducted under this null dispersal model[62] aim to generate a set of lineage dispersal histories (phylogeographic reconstructions) (1) based on the same sampling effort (the same number of samples), (2) maintaining the tree topology and branch lengths (the evolutionary relationships among samples), (3) starting from the same epidemic origin (the location inferred for the most ancestral node of each posterior tree), (4) avoiding non-accessible areas (for example, marine areas) and (5) constrained within the study area (here delimited by the minimum convex hull polygon drawn around all internal and tip node locations retrieved from the set of posterior trees inferred by the continuous phylogeographic analysis). Specifically, the aim of those simulations is therefore to generate a null dispersal model imitating the actual dispersal history but in which the environmental factors have no determined impact on the dispersal location of viral lineages.

From these simulations, values at node positions ($E_{simulated}$) constitute the distribution of mean environmental values explored under a dispersal scenario that is not impacted by any underlying environmental condition. For each environmental factor and segment-specific phylogeographic reconstruction, we then compared the distribution of $E_{estimated}$ values computed from posterior trees with the distribution of $E_{simulated}$ values retrieved from the same tree topologies along which an RRW diffusion process had been resimulated. Specifically, we approximated a BF support equal to $(p_e/(1-p_e))/(0.5/(1-0.5))$. To test if viral lineages tended to avoid circulating within a particular environmental factor e, p_e was defined as the frequency at which $E_{estimated} < E_{simulated}$; and to test if viral lineages tended to preferentially circulate within a particular environmental factor e, p_e was defined as the frequency at which $E_{simulated} < E_{estimated}$. Following the scale of interpretation in ref. 38, we here highlight BF values >20 considered as strong supports.

Ecological niche modelling

Ecological niche models are built using a variety of statistical methods, each varying in complexity and underlying assumptions about the interaction between species occurrences and environmental factors[63]. Recent studies have shown that disparities among different model structures can be very large, making model selection difficult[64]. It is important to note that ecological niche models may achieve comparable performance metrics yet produce very different suitability maps, as also highlighted in ref. 65. An alternative is to use an ensemble of models to avoid selecting one single best model but instead to use a group of methods for inference. In other words, the presence of a species might be well classified by some models and misclassified by others, such that making use of an ensemble model can reduce the predictive uncertainty of a single model by combining predictions[66]. In this study, we applied this approach to investigate the distribution of OROV transmission by creating an ecological suitability map based on the occurrence of OROV disease in Brazil and relevant environmental variables (section on Geospatial Data above). We defined ecological suitability as the output of ecological niche modelling, estimating the likelihood that a given location provides environmental conditions favourable for the potential local circulation of OROV. For this analysis, we aggregate all raster maps to the lowest resolution available (~27 km^2). We used an ensemble of seven statistical, machine learning and envelope models: generalized linear model, generalized additive model, boosted regression trees, RF, classification tree analysis, surface range envelope and maximum entropy model. For RF, we built a conservative RF (500 trees with a maximum depth of 30) to avoid overfitting; detailed parameters for all models are given in Supplementary Table 6. To assess the potential expansion of OROV ecological niche in Brazil during late 2023 and 2024, we computed and compared ecological niche models using occurrence data from different time periods. Specifically, we created three ensemble models using pre-mid-2023 (89 occurrences), pre-2024 (133 occurrences) and the full model with all available occurrence records (450 occurrences).

To assess the performance of the models we use block cross validation[67]. This is a spatially explicit method used to assess model performance by dividing the study area into geographic blocks. Instead of randomly splitting data, this technique ensures that training and testing data are spatially independent, reducing the risk of spatial autocorrelation. TSS and receiver-operating characteristic curve (AUC) are then used to evaluate the predictive performance of the models based on the test (validation) dataset. TSS is equivalent to sensitivity + specificity − 1 and ranges from −1 to 1; value of 1 indicates perfect classification, 0 means the model is no better than random guessing and negative TSS indicates the model performs worse than random guessing. AUC ranges from 0 to 1; AUC of 1 indicates perfect model performance, 0.5 indicates no discrimination (that is, the model is no better than random guessing) and <0.5 indicates the model performs worse than random guessing. We only retained models with a TSS

score of >0.7 to build the ensemble model (Supplementary Fig. 4d). The mean probabilities from each model were then computed and we weighted the predictions of each model according to its performance during training, giving more weight to better-performing models. The weights ensure that higher-quality models contribute more to the final ensemble prediction. The different resulting 'suitability indexes' are then combined to get a single value per site. Once the ensemble predictions are generated, the ensemble model itself is evaluated using the same metrics applied to the individual models; TSS and AUC.

Disease presence points used as input represent OROV circulation occurrence from 450 unique sampling locations in Brazil (molecular testing and sequencing records) from the years 1957 to 2024. Occurrence points with available collection dates were matched to corresponding climatic variables by month. Specifically, temperature and precipitation data for each point were extracted from the monthly climate layers matching the collection month. The sampling of pseudo-absences was done at a 1:1 ratio with presence points[68] and informed by a distribution of presence points and a human population density kernel density estimate. Our aim was to sample absences in proportion to the rate of presence points while giving higher priority to areas with greater population density, ensuring more focused sampling in regions where human populations are denser. This approach helps us to account for disease testing biases in more urbanized areas in the pseudo-absence distribution. Pseudo-absences were also selected within a perimeter of 50–300 km around presence points, ensuring that absence points are neither too close to presence points (to avoid the same niche) or too far (to promote localized sampling strategy). This approach was tested against a random sampling strategy (Supplementary Table 4) for pseudo-absences and after a sensitivity analysis testing the impact of maximum radius distance around presence points (varying from 150 km to 450 km) on model performance (Supplementary Table 5). The minimum distance was kept at 50 km to ensure that pseudo-absence points do not coincide spatially with presence point locations (pixels)[68,69]. This was tested on the full model only.

To determine the independent contributions of each variable to our suitability prediction, we further calculated their RI). Because the RF model demonstrated the highest predictive performance, RI and response curves were derived from this model, whereas the ensemble model was used to build the suitability maps. In the case of RF models, RI is computed by assessing how frequently a variable is selected for splitting at tree nodes, weighted by the squared improvement in model performance resulting from each split and averaged across all trees[70]. Higher RI values indicate greater relative contribution of that variable to the predictive performance of the model. During variable selection, predictors with low contribution or high collinearity with other variables were excluded to avoid redundancy. Forest loss was among the variables removed during this process, as it was strongly correlated with forest cover and did not improve model performance. We also produced response curves to visualize the effect of each variable on suitability predictions in the RF models. These response curves allow us to observe how changes in a single variable influence the predicted outcome, while other variables are held constant (at their mean). By examining these relationships, we gain insights into how each variable individually contributes to the overall predictions of the model.

Reporting summary

Further information on research design is available in the Nature Portfolio Reporting Summary linked to this article.

Data availability

All genomic data used in this study were already openly available before this study (GenBank: PQ149810–PQ149811, PQ247716–PQ247846, PP153945–PP154172 and PQ064571–PQ065491). Disease occurrence data collated here are available via GitHub at https://github.com/CERI-KRISP/OROV_Expansion_Dynamics_Ecology.

Code availability

Analysis scripts are available via GitHub at https://github.com/CERI-KRISP/OROV_Expansion_Dynamics_Ecology.

References

1. Travassos da Rosa, J. F. et al. Oropouche virus: clinical, epidemiological, and molecular aspects of a neglected orthobunyavirus. *Am. J. Trop. Med. Hyg.* **96**, 1019–1030 (2017).
2. About Oropouche. *CDC* https://www.cdc.gov/oropouche/about/index.html (18 September 2025).
3. Barbiero, A. et al. Persistent Oropouche virus viremia in two travellers returned to Italy from Cuba, July 2024. *J. Travel Med.* **32**, taae148 (2025).
4. das Neves Martins, F. E. et al. Newborns with microcephaly in Brazil and potential vertical transmission of Oropouche virus: a case series. *Lancet Infect. Dis.* **25**, 155–165 (2025).
5. Gibrail, M. M. et al. Detection of antibodies to Oropouche virus in non-human primates in Goiânia City, Goiás. *Rev. Soc. Bras. Med. Trop.* **49**, 357–360 (2016).
6. Dye-Braumuller, K. C., Prisco, R. A. & Nolan, M. S. (Re)emerging arboviruses of public health significance in the Brazilian Amazon. *Microorganisms* **13**, 650 (2025).
7. Moreira, H. M. et al. Outbreak of Oropouche virus in frontier regions in western Amazon. *Microbiol. Spectr.* **12**, e0162923 (2024).
8. Sakkas, H., Bozidis, P., Franks, A. & Papadopoulou, C. Oropouche fever: a review. *Viruses* **10**, 175 (2018).
9. Pinheiro, F. P. et al. Oropouche virus. I. A review of clinical, epidemiological, and ecological findings. *Am. J. Trop. Med. Hyg.* **30**, 149–160 (1981).
10. Vasconcelos, H. B. et al. Molecular epidemiology of Oropouche virus, Brazil. *Emerging Infect. Dis.* **17**, 800–806 (2011).
11. Pinheiro, F. P., Travassos da Rosa, A. P., Gomes, M. L., LeDuc, J. W. & Hoch, A. L. Transmission of Oropouche virus from man to hamster by the midge *Culicoides paraensis*. *Science* **215**, 1251–1253 (1982).
12. Roberts, D. R., Hoch, A. L., Dixon, K. E. & Llewellyn, C. H. Oropouche virus. III. Entomological observations from three epidemics in Pará, Brazil, 1975. *Am. J. Trop. Med. Hyg.* **30**, 165–171 (1981).
13. McGregor, B. L., Connelly, C. R. & Kenney, J. L. Infection, dissemination, and transmission potential of North American *Culex quinquefasciatus*, *Culex tarsalis*, and *Culicoides sonorensis* for Oropouche virus. *Viruses* **13**, 226 (2021).
14. Hoch, A. L., Pinheiro, F. P., Roberts, D. R. & Gomes, M. L. Laboratory transmission of Oropouche virus by *Culex quinquefasciatus* Say. *Bull. Pan Am. Health Organ.* **21**, 55–61 (1987).
15. de Mendonça, S. F. et al. Evaluation of *Aedes aegypti*, *Aedes albopictus*, and *Culex quinquefasciatus* mosquitoes competence to Oropouche virus infection. *Viruses* **13**, 755 (2021).
16. de Mendonça, S. F. et al. Oropouche orthobunyavirus in urban mosquitoes: vector competence, coinfection, and immune system activation in *Aedes aegypti*. *Viruses* **17**, 492 (2025).
17. Gallichotte, E. N., Ebel, G. D. & Carlson, C. J. Vector competence for Oropouche virus: a systematic review of pre-2024 experiments. *PLoS Negl. Trop. Dis.* **19**, e0013014 (2025).
18. Oropouche virus disease—region of the Americas. *WHO Disease Outbreak News* https://www.who.int/emergencies/disease-outbreak-news/item/2024-DON530 (23 August 2024).
19. Usuga, J. et al. Co-circulation of 2 Oropouche virus lineages, Amazon Basin, Colombia, 2024. *Emerg. Infect. Dis.* **30**, 2375–2380 (2024).
20. Bandeira, A. C. et al. Fatal Oropouche virus infections in Nonendemic Region, Brazil, 2024. *Emerg. Infect. Dis.* **30**, 2370–2374 (2024).

21. Cola, J. P. et al. Maternal and fetal implications of Oropouche fever, Espírito Santo State, Brazil, 2024. *Emerg. Infect. Dis.* **31**, 645–651 (2025).
22. Braga, A. et al. Oropouche virus infection in pregnancy: emerging evidence on vertical transmission and perinatal outcomes. *J. Matern. Fetal Neonatal Med.* **39**, 2603781 (2026).
23. Naveca, F. G. et al. Human outbreaks of a novel reassortant Oropouche virus in the Brazilian Amazon region. *Nat. Med.* **30**, 3509–3521 (2024).
24. de Melo Iani, F. C. et al. Travel-associated international spread of Oropouche virus beyond the Amazon. *J. Travel Med.* **32**, taaf018 (2025).
25. Moreira, F. R. R. et al. Oropouche virus genomic surveillance in Brazil. *Lancet Infect. Dis.* **24**, e664–e666 (2024).
26. Gräf, T. et al. Expansion of Oropouche virus in non-endemic Brazilian regions: analysis of genomic characterisation and ecological drivers. *Lancet Infect. Dis.* **25**, 379–389 (2025).
27. Delatorre, E. et al. Oropouche virus outbreak in Southeast, Brazil: expanding beyond the Amazonian endemic region. Preprint at *medRxiv* https://doi.org/10.1101/2024.12.11.24318883 (2024).
28. Giovanetti, M. et al. Genomic epidemiology unveils the dynamics and spatial corridor behind the Yellow Fever virus outbreak in Southern Brazil. *Sci. Adv.* **9**, eadg9204 (2023).
29. Files, M. A. et al. Baseline mapping of Oropouche virology, epidemiology, therapeutics, and vaccine research and development. *npj Vaccines* **7**, 38 (2022).
30. Tsui, J. L.-H. et al. Impacts of climate change-related human migration on infectious diseases. *Nat. Clim. Change* **14**, 793–802 (2024).
31. Wesselmann, K. M. et al. Emergence of Oropouche fever in Latin America: a narrative review. *Lancet Infect. Dis.* **24**, e439–e452 (2024).
32. Walsh, C. E. S., Robert, M. A. & Christofferson, R. C. Observational characterization of the ecological and environmental features associated with the presence of Oropouche virus and the primary vector *Culicoides paraenesis*: data synthesis and systematic review. *Trop. Med. Infect. Dis.* **6**, 143 (2021).
33. Romero-Alvarez, D. & Escobar, L. E. Emergent viruses in America: the case of Oropouche virus. *Int. J. Infect. Dis.* **73**, 98 (2018).
34. Aybar, C. A. V., Juri, M. J. D., de Grosso, M. S. L. & Spinelli, G. R. Spatial and temporal distribution of *Culicoides insignis* and *Culicoides paraensis* in the subtropical mountain forest of Tucumán, Northwestern Argentina. *Fla. Entomol.* **94**, 1018–1025 (2011).
35. Gorris, M. E. et al. Updated distribution maps of predominant *Culex* mosquitoes across the Americas. *Parasit. Vectors* **14**, 547 (2021).
36. Cardoso, B. F. et al. Detection of Oropouche virus segment S in patients and in *Culex quinquefasciatus* in the state of Mato Grosso, Brazil. *Mem. Inst. Oswaldo Cruz* **110**, 745–754 (2015).
37. Rozo-Lopez, P., Park, Y. & Drolet, B. S. Effect of constant temperatures on *Culicoides sonorensis* midge physiology and vesicular stomatitis virus infection. *Insects* **13**, 372 (2022).
38. Kass, R. E. & Raftery, A. E. Bayes factors. *J. Am. Stat. Assoc.* **90**, 773–795 (1995).
39. Dellicour, S. et al. Using phylogeographic approaches to analyse the dispersal history, velocity anddirection of viral lineages — application to rabies virus spread in Iran. *Mol. Ecol.* **28**, 4335–4350 (2019).
40. Hoch, A. L., Roberts, D. R. & Pinheiro, F. P. Breeding sites of *Culicoides paraensis* and options for control by environmental management. *Bull. Pan Am. Health Organ.* **20**, 284–293 (1986).
41. Carpenter, S., Groschup, M. H., Garros, C., Felippe-Bauer, M. L. & Purse, B. V. *Culicoides* biting midges, arboviruses and public health in Europe. *Antiviral Res.* **100**, 102–113 (2013).
42. Hoch, A. L. & Roberts, D. R. Host-seeking behavior and seasonal abundance of *Culicoides paraensis* (Diptera: Ceratopogonidae) in Brazil. *J. Am. Mosq. Control Assoc.* **6**, 110–114 (1990).
43. Scachetti, G. C. et al. Re-emergence of Oropouche virus between 2023 and 2024 in Brazil: an observational epidemiological study. *Lancet Infect. Dis.* **25**, 166–175 (2025).
44. Quaglia, S. Clues emerge about an obscure virus' sudden spread. *Science* **386**, 256–257 (2024).
45. Romero-Alvarez, D., Escobar, L. E., Auguste, A. J., Del Valle, S. Y. & Manore, C. A. Transmission risk of Oropouche fever across the Americas. *Infect. Dis. Poverty* **12**, 47 (2023).
46. Gutierrez, B. et al. Evolutionary dynamics of oropouche virus in South America. *J. Virol.* **94**, e01127-19 (2020).
47. Romero-Alvarez, D. & Escobar, L. E. Vegetation loss and the 2016 Oropouche fever outbreak in Peru. *Mem. Inst. Oswaldo Cruz* **112**, 292–298 (2017).
48. Castro, M. C. & Lima Neto, A. S. Unprecedented spread and genetic evolution of the Oropouche virus. *Nat. Med.* **30**, 3420–3421 (2024).
49. Katoh, K., Misawa, K., Kuma, K. & Miyata, T. MAFFT: a novel method for rapid multiple sequence alignment based on fast Fourier transform. *Nucleic Acids Res.* **30**, 3059–3066 (2002).
50. Katoh, K. & Standley, D. M. MAFFT multiple sequence alignment software version 7: improvements in performance and usability. *Mol. Biol. Evol.* **30**, 772–780 (2013).
51. Larsson, A. AliView: a fast and lightweight alignment viewer and editor for large datasets. *Bioinformatics* **30**, 3276–3278 (2014).
52. Martin, D. P. et al. RDP5: a computer program for analyzing recombination in, and removing signals of recombination from, nucleotide sequence datasets. *Virus Evol.* **7**, veaa087 (2021).
53. Poongavanan, J. et al. Spatiotemporal disease suitability prediction for Oropouche virus and the role of vectors across the Americas. Preprint at *medRxiv* https://doi.org/10.1101/2025.02.28.25323068 (2025).
54. Suchard, M. A. et al. Bayesian phylogenetic and phylodynamic data integration using BEAST 1.10. *Virus Evol.* **4**, vey016 (2018).
55. Rambaut, A., Lam, T. T., Max Carvalho, L. & Pybus, O. G. Exploring the temporal structure of heterochronous sequences using TempEst (formerly Path-O-Gen). *Virus Evol.* **2**, vew007 (2016).
56. Lemey, P., Rambaut, A., Welch, J. J. & Suchard, M. A. Phylogeography takes a relaxed random walk in continuous space and time. *Mol. Biol. Evol.* **27**, 1877–1885 (2010).
57. Dellicour, S. Relax, keep walking — a practical guide to continuous phylogeographic inference with BEAST. *Mol. Biol. Evol.* **38**, 3486–3493 (2021).
58. Rambaut, A., Drummond, A. J., Xie, D., Baele, G. & Suchard, M. A. Posterior summarization in Bayesian phylogenetics using Tracer 1.7. *Syst. Biol.* **67**, 901–904 (2018).
59. Dellicour, S., Rose, R., Faria, N. R., Lemey, P. & Pybus, O. G. SERAPHIM: studying environmental rasters and phylogenetically informed movements. *Bioinformatics* **32**, 3204–3206 (2016).
60. Trovão, N. S., Suchard, M. A., Baele, G., Gilbert, M. & Lemey, P. Bayesian inference reveals host-specific contributions to the epidemic expansion of influenza A H5N1. *Mol. Biol. Evol.* **32**, 3264–3275 (2015).
61. Dellicour, S. et al. How fast are viruses spreading in the wild? *PLoS Biol.* **22**, e3002914 (2024).
62. Dellicour, S. et al. Phylodynamic assessment of intervention strategies for the West African Ebola virus outbreak. *Nat. Commun.* **9**, 2222 (2018).
63. Merow, C., Smith, M. J. & Silander, J. A. A practical guide to MaxEnt for modeling species' distributions: what it does, and why inputs and settings matter. *Ecography* **36**, 1058–1069 (2013).
64. Guisan, A., Thuiller, W. & Zimmermann, N. E. *Habitat Suitability and Distribution Models: With Applications in R* (Cambridge Univ. Press, 2017).

65. Singleton, A. L. et al. Species distribution modeling for disease ecology: a multi-scale case study for schistosomiasis host snails in Brazil. *PloS Glob. Public Health* **4**, e0002224 (2024).
66. Marmion, M., Parviainen, M., Luoto, M., Heikkinen, R. K. & Thuiller, W. Evaluation of consensus methods in predictive species distribution modelling. *Divers. Distrib.* **15**, 59–69 (2009).
67. Muscarella, R. et al. ENMeval: an R package for conducting spatially independent evaluations and estimating optimal model complexity for Maxent ecological niche models. *Methods Ecol. Evol.* **5**, 1198–1205 (2014).
68. Barbet-Massin, M., Jiguet, F., Albert, C. H. & Thuiller, W. Selecting pseudo-absences for species distribution models: how, where and how many?. *Methods Ecol. Evol.* **3**, 327–338 (2012).
69. Chefaoui, R. M. & Lobo, J. M. Assessing the effects of pseudo-absences on predictive distribution model performance. *Ecol. Model.* **210**, 478–486 (2008).
70. Gregorutti, B., Michel, B. & Saint-Pierre, P. Correlation and variable importance in random forests. *Stat. Comput.* **27**, 659–678 (2017).

Acknowledgements

We would like to acknowledge F. G. Naveca for the diagnostic-based approach developed, which enabled the detection of OROV across Brazil and the Americas. Research at CERI was supported by the South African Medical Research Council (SAMRC) with funds received from the National Department of Health. Modelling activities at KRISP and CERI are supported in part by grants from the Rockefeller Foundation (HTH 017), the Abbott Pandemic Defense Coalition (APDC), the National Institute of Health USA (U01 AI151698) for the United World Antivirus Research Network (UWARN), the INFORM Africa project through IHVN (U54 TW012041) and the eLwazi Open Data Science Platform and Coordinating Center (U2CEB032224), the SAMRC South African mRNA Vaccine Consortium (SAMVAC), European Union supported by the Global Health EDCTP3 Joint Undertaking and its members as well as Bill & Melinda Gates Foundation (101103171), European Union's Horizon Europe Research and Innovation Programme (101046041), the Health Emergency Preparedness and Response Umbrella Program (HEPR Program), managed by the World Bank Group (TF0B8412), the GIZ commissioned by the Government of the Federal Republic of Germany, the UK Medical Research Foundation (MRF-RG-ICCH-2022-100069, also supporting M.U.G.K.), the Wellcome Trust for the Global.health project (228186/Z/23/Z, also supporting M.U.G.K.) and the Novo Nordisk Foundation (NNF24OC0094346, also supporting M.U.G.K. and M.G.). This study was also supported by the National Institutes of Health USA grant no. U01 AI151698 for the United World Arbovirus Research Network (UWARN), the CRP-ICGEB RESEARCH GRANT 2020 Project CRP/BRA20-03, contract CRP/20/03 and the Rede Unificada de Análises Integradas de Arbovírus de Minas Gerais (REDE UAI-ARBO-MG), financed by Fundação de Amparo à Pesquisa do Estado de Minas Gerais (FAPEMIG), grant no. RED-00234-23. S.D. acknowledges support from the *Fonds National de la Recherche Scientifique* (F.R.S.-FNRS, Belgium; grant no. F.4515.22), from the Université Libre de Bruxelles internal found, from the Research Foundation—Flanders (*Fonds voor Wetenschappelijk Onderzoek*—Vlaanderen, FWO, Belgium; grant no. G098321N) and from the European Union Horizon 2020 project LEAPS (grant agreement no. 101094685). Funding for M.G. is provided by PON 'Ricerca e Innovazione' 2014–2020. The content and findings reported herein are the sole deduction, view and responsibility of the researcher/s and do not reflect the official position and sentiments of the funding agencies. E.C.H. is supported by a National Health and Medical Research Council (NHMRC) Investigator award (GNT2017197) and by AIR@InnoHK administered by the Innovation and Technology Commission, Hong Kong Special Administrative Region, China. The authors gratefully acknowledge the Global Consortium to Identify and Control Epidemics—CLIMADE (https://climade.health/). M.U.G.K. acknowledges funding from The Rockefeller Foundation (PC-2022-POP-005), Google.org, the Oxford Martin School Programmes in Pandemic Genomics & Digital Pandemic Preparedness, European Union Horizon Europe programme projects MOOD (no. 874850) and E4Warning (no. 101086640), the John Fell Fund, a Branco Weiss Fellowship and Wellcome Trust grants no. 225288/Z/22/Z, 226052/Z/22/Z, United Kingdom Research and Innovation (no. APP8583). J.L. acknowledges the Fundação para a Ciência e Tecnologia (FCT) for institutional support to his host institution, CBR (DOI:10.54499/UID/06497/2025, UID/06497/2025). V.F. was supported by the Conselho Nacional de Desenvolvimento Científico e Tecnológico (CNPq), Brazil [grant number 444903/2024-0 and 314941/2025-8].

Author contributions

Contact for the Consortium CLIMADE: ceri@sun.ac.za. Conceptualization: H.T., T.d.O. Methodology: H.T., S.D., C.M., G.D., V.F., M.S.T., M.D., L.C.V.F., C.F.C.d.A., M.M., E.W., E.C.H., C.B., R.L., M.U.G.K., J.L., L.C.J.A., T.d.O., M.G. Investigation: H.T., S.D., J.P., C.M., V.F., J.L., M.G. Data curation: H.T., J.P., M.G. Writing—original draft: H.T., S.D., J.P., C.M., J.L., M.U.G.K., T.d.O., M.G. Visualization: H.T., S.D., J.P. Funding acquisition: T.d.O., L.C.J.A., M.G. All authors have read and agreed to the published version of the paper.

Competing interests

The authors declare no competing interests.

Additional information

Supplementary information The online version contains supplementary material available at https://doi.org/10.1038/s41559-026-03042-0.

Correspondence and requests for materials should be addressed to Houriiyah Tegally, Tulio de Oliveira or Marta Giovanetti.

Peer review information *Nature Ecology & Evolution* thanks the anonymous reviewers for their contribution to the peer review of this work.

[1]Centre for Epidemic Response and Innovation (CERI), School of Data Science and Computational Thinking, Stellenbosch University, Stellenbosch, South Africa. [2]Spatial Epidemiology Lab (SpELL), Université Libre de Bruxelles, Brussels, Belgium. [3]Department of Microbiology, Immunology and Transplantation, Rega Institute, KU Leuven, Leuven, Belgium. [4]Interuniversity Institute of Bioinformatics in Brussels, Université Libre de Bruxelles, Vrije Universiteit Brussel, Brussels, Belgium. [5]Emerging Pathogens Institute, Department of Pathology, College of Medicine, University of Florida, Gainesville, FL, USA. [6]Global Health Program Smithsonian's National Zoo & Conservation Biology Institute, Washington, DC, USA. [7]Global Health Institute, University of Wisconsin-Madison, Madison, WI, USA. [8]Department of Exact and Earth Science, University of the State of Bahia, Salvador, Brazil. [9]Instituto René Rachou, Fundação Oswaldo Cruz, Belo Horizonte, Brazil. [10]Interdisciplinary Center for Biotechnology Research, University of Florida, Gainesville, FL, USA. [11]Computer Science Division, Department of Mathematical Sciences, Stellenbosch University, Stellenbosch, South Africa. [12]Organização Pan-Americana da Saúde/Organização Mundial da Saúde, Brasília, Brazil. [13]Coordenadora-Geral de Vigilância de Arboviroses, Brazilian Ministry of Health, Brasília, Brazil. [14]School of Medical Sciences, University of Sydney, Sydney, New South Wales, Australia. [15]KwaZulu-Natal Research Innovation and Sequencing Platform (KRISP), Nelson R Mandela School of Medicine, University of KwaZulu-Natal, Durban, South Africa. [16]Pandemic Sciences Institute, University of Oxford, Oxford, UK. [17]Department of Biology, University of Oxford, Oxford, UK. [18]Universidade Católica Portuguesa, Católica Medical School, Católica Biomedical Research Center, Lisbon, Portugal. [19]Oswaldo Cruz Institute, Oswaldo Cruz Foundation, Rio de Janeiro, Brazil. [20]Department of Science and Bio-Technology, Università Campus Bio-Medico di Roma, Rome, Italy. [53]These authors contributed equally: Houriiyah Tegally, Simon Dellicour, Jenicca Poongavanan, Carla Mavian. [54]These authors jointly supervised this work: Tulio de Oliveira, Marta Giovanetti. *A list of authors and their affiliations appears at the end of the paper. ✉e-mail: houriiyah@sun.ac.za; tulio@sun.ac.za; giovanetti.marta@gmail.com

Consortium CLIMADE

Tulio de Oliveira[1], Luiz C. J. Alcantara[9], Edward C. Holmes[14], Abdou Padane[21], Abdualmoniem O. A. Musa[22,23], Adugna Abera[24], Allan Campbell[25], Aloysious Ssemaganda[26], Ambroise Ahouidi[21], Argentina F. Muianga[27], Aziza John Samson[28], Anyebe Bernard Onoja[29], Badara Cissé[21], Birhanu D. Alemu[30], Carlin Foka[1], Cheryl Baxter[1], Daniel van Zyl[1], Danilo de Castro Silva[1], Darren Martin[31], Desalew M. Moges[1], Eduan Wilkinson[1], Carla Mavian[1], Eninam Kouma[32], Fredy B. N. Simo[33], Gaspary Mwanyika[1], Girma Godebo[34], Graeme D'or[1], Houriiyah Tegally[1,53], Isaac Emmanuel Omara[1], James Ayei Maror[35], Jennica Poonagavan[1], John Juma[36], John Oludele[27], Joicymara S. Xavier[1,37], José Lourenço[18], Joseph Fokam[38], Kenneth K. Maeka[39], Lavanya Singh[1], Lucious Chabuka[1], Maman Issaka[32], Marije Hofstra[1], Marta Giovanetti[19,20,40], Martin Faye[41], Melissa Ahou Koffi[42], Michael Owusu[43], Michel N. Dikongo[44], Mohamed Z. Alimohamed[45], Molalegne Bitew[46], Monika Moir[1], Moritz U. G. Kraemer[16,17], Nikita Sitharam[1], Nkurunziza Jerome[47], Nokuzola Mbhele[31], Ny Haingo Miantsatian Andry[1], Oyewale Tomori[48], Ramuth Magalutcheemee[49], Ronison Alves Guimaraes[50], Samuel Oyola[36], Sara A. Abuelmaali[51], Souleymane Mboup[21], Tanya Golubchik[14], Vagner Fonseca[1,8,9], Wolfgang Preiser[52] & Yajna Ramphal[1]

[21]Institute de Recherche en Santé, de Surveillance Épidémiologique et de Formations (IRESSEF), Rufisque, Senegal. [22]Faculty of Medical Laboratory Sciences, University of Kassala, Kassala City, Sudan. [23]General Administration of Laboratories and Blood Banks, Ministry of Health, Khartoum, Sudan. [24]Malaria and Neglected Tropical Diseases Research Team, Ethiopian Public Health Institute, Addis Ababa, Ethiopia. [25]Central Public Health Reference Laboratory, Freetown, Sierra Leone. [26]National Health Laboratories and Diagnostic Services, Central Public Health Laboratories, Kampala, Uganda. [27]Instituto Nacional de Saude, Marracuene, Mozambique. [28]National Institute for medical research (NIMR), Dodoma, Tanzania. [29]University of Ibadan, Ibadan, Nigeria. [30]PATH, Addis Ababa, Ethiopia. [31]University of Cape Town, Cape Town, South Africa. [32]Institut National d'Hygiène, Lomé, Togo. [33]Centre for Research in Infectious Disease, CRID, Yaoundé, Cameroon. [34]Wachemo University, Hossana, Ethiopia. [35]National Public Health Laboratory, Juba, South Sudan. [36]International Livestock Research Institute (ILRI), Nairobi, Kenya. [37]Department of Software and Information Systems, Computer Science Division, Instituto Tecnológico de Aeronáutica (ITA), São José dos Campos, São Paulo, Brazil. [38]Chantal BIYA International Reference Centre (CIRCB), Faculty of Medicine and Biomedical Sciences of the University of Yaounde I, National AIDS Control Committee, Yaounde, Cameroon. [39]National Microbiology Reference Laboratory, Ministry of Health, Harare, Zimbabwe. [40]Laboratório de Flavivírus, Instituto Oswaldo Cruz, Fundação Oswaldo Cruz, Rio de Janeiro, Brazil. [41]Institute Pasteur de Dakar, Dakar, Senegal. [42]Département des Virus Epidémiques, Abidjan, Côte d'Ivoire. [43]Kwame Nkrumah University of Science and Technology, Kumasi, Ghana. [44]Independent researcher, Franceville, Gabon. [45]Muhimbili University of Health and Allied Sciences, Dar es Salaam, Tanzania. [46]Health Biotechnology Directorate, Bio and Emerging Technology Institute, Addis Ababa, Ethiopia. [47]Hope Africa University, National Institute of Public Health Reference Laboratory, Bujumbura, Burundi. [48]African Centre of Excellence for Genomics of Infectious Diseases (ACEGID), Redeemer's University, Ede, Nigeria. [49]Virology Department, Central Health Laboratory, Ministry of Health and Wellness, Candos, Mauritius. [50]Federal University of Minas Gerais, Belo Horizonte, Brazil. [51]National Public Health Laboratory, Khartoum, Sudan. [52]University of Stellenbosch / National Health Laboratory Service, Tygerberg, South Africa.

nature portfolio

Corresponding author(s): Carla Mavian

Last updated by author(s): Jan 13, 2026

Reporting Summary

Nature Portfolio wishes to improve the reproducibility of the work that we publish. This form provides structure for consistency and transparency in reporting. For further information on Nature Portfolio policies, see our Editorial Policies and the Editorial Policy Checklist.

Statistics

For all statistical analyses, confirm that the following items are present in the figure legend, table legend, main text, or Methods section.

n/a	Confirmed
☐	☒ The exact sample size (*n*) for each experimental group/condition, given as a discrete number and unit of measurement
☐	☒ A statement on whether measurements were taken from distinct samples or whether the same sample was measured repeatedly
☐	☒ The statistical test(s) used AND whether they are one- or two-sided *Only common tests should be described solely by name; describe more complex techniques in the Methods section.*
☐	☒ A description of all covariates tested
☒	☐ A description of any assumptions or corrections, such as tests of normality and adjustment for multiple comparisons
☐	☒ A full description of the statistical parameters including central tendency (e.g. means) or other basic estimates (e.g. regression coefficient) AND variation (e.g. standard deviation) or associated estimates of uncertainty (e.g. confidence intervals)
☐	☒ For null hypothesis testing, the test statistic (e.g. *F*, *t*, *r*) with confidence intervals, effect sizes, degrees of freedom and *P* value noted *Give P values as exact values whenever suitable.*
☐	☒ For Bayesian analysis, information on the choice of priors and Markov chain Monte Carlo settings
☒	☐ For hierarchical and complex designs, identification of the appropriate level for tests and full reporting of outcomes
☒	☐ Estimates of effect sizes (e.g. Cohen's *d*, Pearson's *r*), indicating how they were calculated

Our web collection on statistics for biologists contains articles on many of the points above.

Software and code

Policy information about availability of computer code

Data collection	In this study, all OROV genome sequences, along with related metadata, were obtained from the open-source Genbank platform. No software was used specifically for data collection.
Data analysis	Data analysis involved the use of a range of open-source bioinformatics and phylogenetic tools. Sequence alignment was performed using MAFFT and subsequently curated manually to remove artefacts using AliView 51. Genomic regions were screened for recombination using RDP5. We performed Bayesian phylogenetic and phylogeographic analyses using software package BEAST 1.10 after testing the molecular clock signal of our dataset using TempEst v1.5.3. Maximum clade credibility trees were summarised using TreeAnnotator after discarding burn-in samples, the number of which was also determined in the software Tracer. Finally, the R package “seraphim” was employed to extract and map the spatiotemporal information embedded in the posterior trees, and to perform landscape phylogeographic testing. For ecological niche modelling, we used an ensemble of seven statistical, machine learning, and envelope models: Generalised Linear Model (GLM), Generalised Additive Model (GAM), Boosted Regression Trees (BRT), Random Forest (RF), Classification Tree Analysis (CTA), Surface Range Envelope (SRE) and Maximum Entropy Model (MAXENT), implemented in R. For plotting maps, we used shapefiles from the package "rnaturalearth" in R. Additional visualizations were made using the R packages ggplot2. The scripts and code used for the analysis are available in our GitHub repository: https://github.com/CERI-KRISP/OROV_Expansion_Dynamics_Ecology

For manuscripts utilizing custom algorithms or software that are central to the research but not yet described in published literature, software must be made available to editors and reviewers. We strongly encourage code deposition in a community repository (e.g. GitHub). See the Nature Portfolio guidelines for submitting code & software for further information.

Data

Policy information about availability of data

All manuscripts must include a data availability statement. This statement should provide the following information, where applicable:

- Accession codes, unique identifiers, or web links for publicly available datasets
- A description of any restrictions on data availability
- For clinical datasets or third party data, please ensure that the statement adheres to our policy

All genomic data used in this study were already openly available before this study (Genbank: PQ149810-PQ149811, PQ247716-PQ247846, PP153945-PP154172, and PQ064571-PQ065491). Disease occurrence data collated here and analysis scripts are made openly available at: https://github.com/CERI-KRISP/OROV_Expansion_Dynamics_Ecology .

Research involving human participants, their data, or biological material

Policy information about studies with human participants or human data. See also policy information about sex, gender (identity/presentation), and sexual orientation and race, ethnicity and racism.

Reporting on sex and gender	No reporting on sex and/or gender was performed in this study
Reporting on race, ethnicity, or other socially relevant groupings	No reporting on race, ethnicity, or other socially relevant groupings was performed in this study
Population characteristics	This study did not involve human research participants directly.
Recruitment	This study did not involve human research participants directly.
Ethics oversight	This study did not involve human research participants directly.

Note that full information on the approval of the study protocol must also be provided in the manuscript.

Field-specific reporting

Please select the one below that is the best fit for your research. If you are not sure, read the appropriate sections before making your selection.

☐ Life sciences ☐ Behavioural & social sciences ☒ Ecological, evolutionary & environmental sciences

For a reference copy of the document with all sections, see nature.com/documents/nr-reporting-summary-flat.pdf

Ecological, evolutionary & environmental sciences study design

All studies must disclose on these points even when the disclosure is negative.

Study description	This observational study integrates phylogeographic and ecological niche modelling techniques to understand the evolutionary and ecological drivers of Oropouche virus expansion in Brazil in 2024.
Research sample	The research sample consists of 545 genome sequences of Oropouche virus segments (S, L and L), along with related metadata, that were available on the Genbank database, along with Oropouche occurrence data points curated from available literature.
Sampling strategy	Genomic data was selected to represent the re-emerging outbreak of Oropouche in 2024 in Brazil. Disease occurrence data was curated from all available public records for this virus from 1957 to 2024.
Data collection	All genomic data used in this study were already openly available before this study (Genbank: PQ149810-PQ149811, PQ247716-PQ247846, PP153945-PP154172, and PQ064571-PQ065491). Disease occurrence data collated here and analysis scripts are made openly available at: https://github.com/CERI-KRISP/OROV_Expansion_Dynamics_Ecology.
Timing and spatial scale	The genomic data used in this study spanned from August 2023 to May 2024, and represented geocoded locations in 9 states of Brazil. Disease occurrence data spanned the years 1957 to 2024, representing geocoded locations all over Brazil.
Data exclusions	Sequences with recombination and reassortment signals along the majority of the genome were completely discarded (n=43 for segment S and n=1 for segment L).
Reproducibility	To ensure reproducibility of the findings, the study utilised widely accessible open-source tools and methodologies. The methods outlining the data acquisition and analysis are described in detail. All relevant scripts and additional curated data have been uploaded to our GitHub repository (https://github.com/CERI-KRISP/OROV_Expansion_Dynamics_Ecology).

Randomization	Randomisation, in its technical sense, was not relevant to this study.
Blinding	Blinding was not relevant to this study.

Did the study involve field work? ☐ Yes ☒ No

Reporting for specific materials, systems and methods

We require information from authors about some types of materials, experimental systems and methods used in many studies. Here, indicate whether each material, system or method listed is relevant to your study. If you are not sure if a list item applies to your research, read the appropriate section before selecting a response.

Materials & experimental systems

n/a	Involved in the study
☒	☐ Antibodies
☒	☐ Eukaryotic cell lines
☒	☐ Palaeontology and archaeology
☒	☐ Animals and other organisms
☒	☐ Clinical data
☒	☐ Dual use research of concern
☒	☐ Plants

Methods

n/a	Involved in the study
☒	☐ ChIP-seq
☒	☐ Flow cytometry
☒	☐ MRI-based neuroimaging

Plants

Seed stocks	*Report on the source of all seed stocks or other plant material used. If applicable, state the seed stock centre and catalogue number. If plant specimens were collected from the field, describe the collection location, date and sampling procedures.*
Novel plant genotypes	*Describe the methods by which all novel plant genotypes were produced. This includes those generated by transgenic approaches, gene editing, chemical/radiation-based mutagenesis and hybridization. For transgenic lines, describe the transformation method, the number of independent lines analyzed and the generation upon which experiments were performed. For gene-edited lines, describe the editor used, the endogenous sequence targeted for editing, the targeting guide RNA sequence (if applicable) and how the editor was applied.*
Authentication	*Describe any authentication procedures for each seed stock used or novel genotype generated. Describe any experiments used to assess the effect of a mutation and, where applicable, how potential secondary effects (e.g. second site T-DNA insertions, mosiacism, off-target gene editing) were examined.*